Explanation of Photon Correlations in the Far-Off-Resonance Optical Emission from a Quantum-Dot–Cavity System

Martin Winger,[1] Thomas Volz,[1] Guillaume Tarel,[2] Stefano Portolan,[2] Antonio Badolato,[3] Kevin J. Hennessy,[4] Evelyn L. Hu,[4] Alexios Beveratos,[5] Jonathan Finley,[6] Vincenzo Savona,[2] and Ataç Imamoğlu[1]

[1]*Institute of Quantum Electronics, ETH Zurich, 8093 Zurich, Switzerland*
[2]*Institute of Theoretical Physics, Ecole Polytechnique Fédérale de Lausanne EPFL, CH-1015 Lausanne, Switzerland*
[3]*Department of Physics and Astronomy, University of Rochester, Rochester, New York 14627, USA*
[4]*California NanoSystems Institute, University of California, Santa Barbara, California 93106, USA*
[5]*CNRS–Laboratoire Photonique et Nanostructures, Route de Nozay, F-91460 Marcoussis, France*
[6]*Walter Schottky Institut, Am Coulombwall 3, D-85748 Garching, Germany*

(Received 21 August 2009; published 12 November 2009)

In a coupled quantum-dot–nanocavity system, the photoluminescence from an off-resonance cavity mode exhibits strong quantum correlations with the quantum-dot transitions, even though its autocorrelation function is classical. Using new pump-power dependent photon-correlation measurements, we demonstrate that this seemingly contradictory observation that has so far defied an explanation stems from cascaded cavity photon emission in transitions between excited multiexciton states. The mesoscopic nature of quantum-dot confinement ensures the presence of a quasicontinuum of excitonic transitions, part of which overlaps with the cavity resonance.

DOI: 10.1103/PhysRevLett.103.207403 PACS numbers: 78.67.Hc, 42.50.Pq

A quantum dot (QD) coupled to a photonic crystal cavity provides a promising system for studying cavity quantum-electrodynamics (QED) in the solid state [1,2]. In contrast to their atom-based counterparts, these systems exhibit features that arise from their complex environment. A common effect that surfaced in previous experiments is strong off-resonant emission of a cavity mode (CM) containing one or multiple QDs. Photon-correlation measurements revealed that the cavity-mode emission is anticorrelated with the QD excitons at the level of single quanta, proving that cavity feeding is mediated solely by a single QD [3,4]. Surprisingly, however, the photon stream emitted by the far off-resonant CM did not show any significant quantum correlations. Previous experimental [5–7] and theoretical [8,9] investigations have focused on explaining cavity feeding in terms of dephasing of the QD excitons mediated either by coupling to acoustic phonons or to free carriers. However, all of the attempts to describe cavity feeding using Markovian dephasing of the fundamental exciton line fail to explain the above mentioned photon-correlation signatures that appear to be true for all studied QD-cavity–QED systems.

In this Letter, we unequivocally demonstrate that the far off-resonant excitation of the CM is solely due to the mesoscopic nature of quantum-dot confinement, which in turn leads to an energetically broad cascaded emission of the QD. In this setting, cavity feeding and its photon-correlation signatures can be regarded as an intrinsic feature of QD-cavity systems that arises from the complicated QD multiexciton level structure. We carry out pump-power dependent photoluminescence (PL) as well as photon auto- and cross-correlation measurements on a nanostructure incorporating a single QD embedded in a photonic crystal (PC) defect cavity [3]. To explain our experimental observations, we develop a new theoretical model for the QD-cavity system, perform numerical calculations of its semiclassical dynamics, and compare its predictions with the new experimental findings. While a quantitative comparison between numerical and experimental results is intrinsically difficult, the qualitative agreement we achieve is excellent. In particular, the unusual correlation features found experimentally are naturally reproduced by the model and the simulations.

Before proceeding, we remark that acoustic phonons should contribute to cavity feeding [10] when the CM-exciton detuning does not exceed a cutoff energy determined by the inverse QD size, typically in the range of 1 meV (0.7 nm). In contrast, cavity feeding has experimentally been observed for detunings ranging from $+10$ meV (-7 nm) to -45 meV ($+32$ nm) (i.e., $\sim$70–300 CM linewidths). Our focus in this Letter lies on this far off-resonance cavity emission phenomenon, which cannot be explained using (Markovian) pure-dephasing or phonon-assisted processes.

A key aspect of cavity feeding can be identified from typical PL spectra of a single QD coupled to a PC cavity. Figure 1(a) displays a PL spectrum of such a device on a semilogarithmic scale with a cavity-mode frequency tuned about 15.3 meV (10.9 nm) red of the X^0 transition using nitrogen deposition [11,12]. The spectrum was obtained in a liquid-helium flow cryostat by pumping the device at around 838 nm, just below the GaAs band gap. Even though the QD is driven well below saturation, the CM emission is clearly visible together with the dominant QD

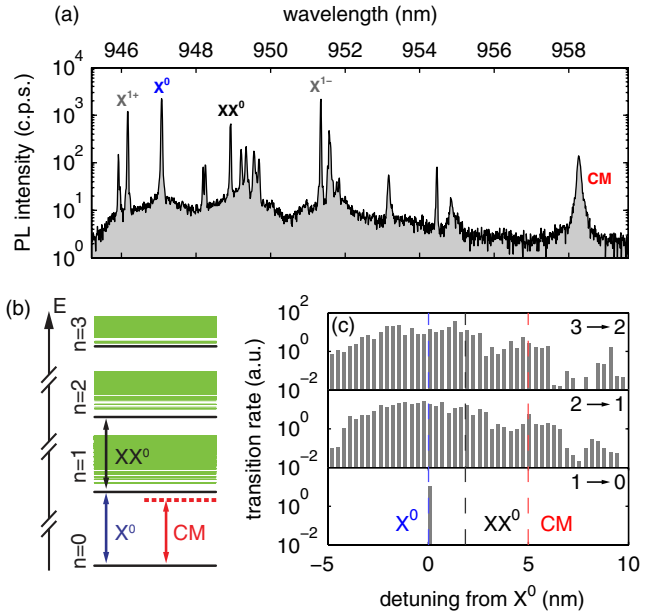

FIG. 1 (color online). QD background emission and level structure. (a) Typical QD PL spectrum on a semilogarithmic scale. Besides the well-known discrete QD lines, the weak background responsible for cavity feeding is visible. (b) Calculated energy-level diagram ($n \leq 3$) of a neutral QD assuming a truncated parabolic in-plane confinement potential (energy separations between manifolds not to scale). (c) Calculated transition rates between states of different manifolds. States from $n \geq 2$ manifolds can decay into a large number of final states, thus forming a quasicontinuum of allowed transitions that can feed the CM.

PL lines that originate mainly from the neutral exciton X^0, the negatively (X^{1-}) and positively (X^{1+}) charged trions, and the biexciton (XX^0) transition [13]. We remark here that for our devices and excitation conditions, the magnitude of X^0, X^{1-}, and X^{1+} are comparable, suggesting that the QD is equally likely to be neutral or charged by a single excess electron or a hole. In addition to these discrete lines, we observe a much broader single-QD background about 2 orders of magnitude weaker in intensity. The part of this background that is resonant with the CM is Purcell enhanced and leads to the off-resonant cavity luminescence.

To understand this single-QD background emission, we consider the full excitation spectrum of electron and hole motional states in the QD. While the narrow QD lines originate from states in which the carriers occupy lowest energy single-particle states, there is a large variety of higher excited states for which, e.g., a carrier is excited to a p- or d-shell state. This leads to an excitation spectrum consisting of a series of QD manifolds separated approximately by the band-gap energy. We calculate the multiexcitonic eigenstates up to four electron-hole pairs [14,15] by diagonalizing the Coulomb Hamiltonian, starting from a basis of 18 electron and 32 hole states including spin. The result of the calculation is displayed in Fig. 1(b). This configuration interaction approach is able to catch the relevant Coulomb correlations that would otherwise require a many-body density matrix treatment [16]. In particular, it has recently been demonstrated that higher energy orbital states in an excitation manifold n (with $n \geq 2$ electron-hole pairs) are subject to strong hybridization with the wetting-layer continua [17]. This leads to the formation of a continuum of QD excited states for each n. In this more accurate picture for the QD spectrum, the X^0 line corresponds to a transition from the lowest energy $n = 1$ manifold state to the ground state ($1 \rightarrow 0$), whereas XX^0 decay relates to a transition between the lowest energy states of the $n = 2$ and $n = 1$ manifolds ($2 \rightarrow 1$) [Fig. 1(b)]. Given the large variety of initial and final states, $2 \rightarrow 1$ (and higher manifold) transitions merge to a quasicontinuum and give rise to QD background emission that feeds the CM [18]. Figure 1(c) shows calculated transition rates between states of different manifolds. For initial states in manifolds $n \geq 2$, decay can occur over a wide spectral range, while decay from $n = 1$ states leads to a series of discrete emission lines, with the first excited transition ~30 meV (21 nm) blue detuned from the X^0 line [not visible in Fig. 1(c)]. We note that similar excitation spectra exist for a charged QD. In contrast to the X^0 level spectrum, here also the $n = 0^{\pm}$ manifolds consist of multiple states owing to the excited confined motional states of the extra charge. Hence, for charged QDs cavity feeding can also occur for $1^{\pm} \rightarrow 0^{\pm}$ transitions.

Because of the excited-state nature of cavity feeding for a neutral QD, we expect a superlinear pump-power dependence of the CM emission. In Fig. 2(a), we show the integrated intensities of the CM together with those of the X^0, X^{1-}, and XX^0 lines as a function of pump power in a log-log plot. As expected, the X^0 and X^{1-} lines follow an approximately linear power dependence below satura-

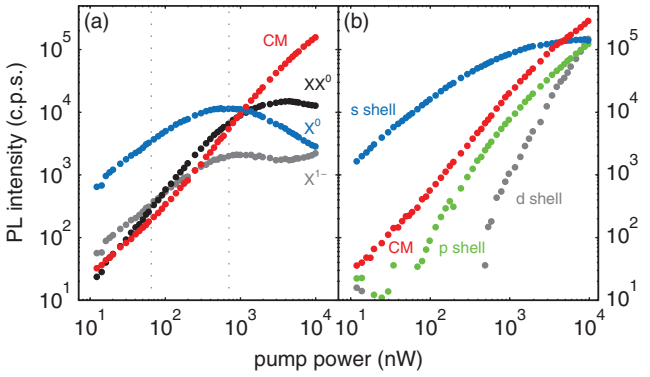

FIG. 2 (color). Off-resonant cavity emission as a function of pump power. (a) Pump-power dependence of CM, X^0, X^{1-}, and XX^0 emission. The data were obtained by integrating PL intensities for different excitation powers in ≈ 0.3 nm wide windows around the different QD lines indicated in Fig. 1(a). The CM exhibits complex dynamics due to cavity feeding from higher-lying multiexcitonic states. (b) Comparison of CM emission with the emission from the different QD shells. The CM dynamics is clearly dominated by the QD s shell for powers below 500 nW, while at higher powers the p shell takes over.

tion (which is defined through the emission maximum of the respective line). A power-law fit to the XX^0 data gives an exponent of ~ 1.5. In contrast, the dynamics of the CM is more complex. For pump powers below ~ 100 nW, the CM follows a linear dependence, similar to the X^0 and the X^{1-}. This observation is consistent with our model since for very low pump powers we expect the charged $1^{\pm} \rightarrow 0^{\pm}$ exciton transitions to give the dominant contribution to cavity feeding. When increasing the pump power, the behavior of the CM emission becomes superlinear: in between the two vertical lines in Fig. 2(a), the cavity displays the power dependence of the XX^0 line. Furthermore, the cavity intensity increases far above the saturation levels of both the X^0 and the XX^0. For powers above 500 nW, the cavity luminescence follows that of the QD p-shell as clearly demonstrated in Fig. 2(b). Here we recorded PL data over a wide spectral window covering the QD s, p, and d shells and plot the total integrated intensity of the shell emissions as a function of pump power. Since p- and d-shell emissions originate from higher-excitation manifolds of the QD [19], these observations strongly support our model of cavity feeding.

As argued earlier, the most striking feature of cavity feeding is the peculiar interplay of quantum correlations observed in off-resonant cavity PL [3,4]. To obtain a better understanding of these observations, we carried out pump-power dependent photon-correlation measurements that show new features that were not visible in earlier measurements. Figures 3(a)–3(c) display normalized CM-X^0 cross-correlation curves for a mutual detuning of about 10.3 meV (7.3 nm) for three different pump powers. The histograms

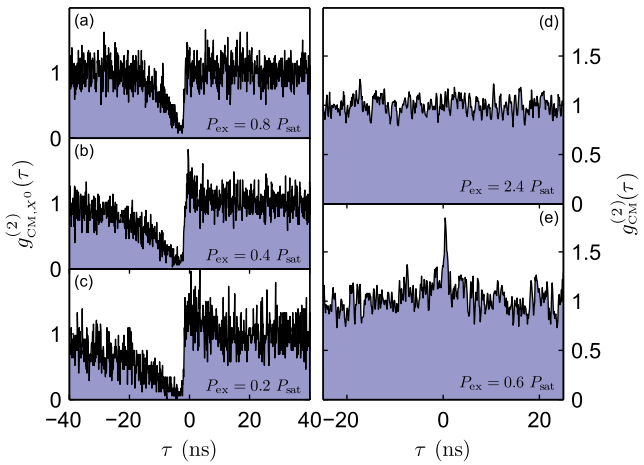

FIG. 3 (color online). Experimental correlation histograms. (a)–(c) Cross correlations between the CM and the X^0 for different pump powers. $\tau > 0$ refers to X^0 emission upon detection of a cavity photon. The bunching feature for $\tau > 0$ disappears when increasing the pump power, as expected from our model. The time scale for the antibunching feature for negative delays reflects the repump time of the system. (d)–(e) CM autocorrelations for two different pump powers. Below saturation, clear bunching at $\tau = 0$ is visible which disappears above saturation, in agreement with the model.

were taken at pump powers of about (c) 20%, (b) 40%, and (a) 80% of the saturation power $P_{sat} \approx 600$ nW. For all three pump powers, there is a strong suppression of coincidences for zero time delay. In other words, CM and X^0 emission do not occur simultaneously, which follows naturally from our model since cavity feeding arises from QD transitions other than the X^0. Moreover, we observe an abrupt turn-on of X^0 luminescence upon detection of a cavity photon, reflected by the bunching feature for $\tau > 0$. This can easily be explained by the fact that for pump powers below saturation, a significant portion of cavity photons is emitted in $2 \rightarrow 1$ transitions. In this case, detection of a cavity photon projects the QD into the $n = 1$ manifold, leading to a higher-than-average probability for X^0 emission. When increasing the pump power, the average QD population is higher, such that the detection of a cavity photon does not increase the conditional probability that the QD is in the $n = 1$ manifold. This is manifested in a reduction and eventually the disappearance of the bunching peak for higher powers, as clearly visible in Figs. 3(a) and 3(b) [20].

Surprisingly, in our previous study the cavity photons did not show any significant quantum correlations [3] even though the cavity is fed by a single quantum emitter. To gain further insight, we measure the second-order autocorrelation function $g^{(2)}_{CM}(\tau)$ of the cavity luminescence for different pump powers. Here, the cavity is detuned by 15.3 meV (10.9 nm) to the red of the X^0. Figures 3(d) and 3(e) display the outcome for two different regimes of pump powers. While for a pump power $P_{ex} \approx 0.6 P_{sat}$ [Fig. 3(e)] the cavity emission exhibits clear bunching for $\tau = 0$, well above saturation the bunching disappears and the correlations are purely Poissonian [Fig. 3(d)]. We argue that the observation of bunching, not observed in earlier single-QD experiments, provides a strong indication of cavity feeding from QD excited states as predicted by our model: when the system is driven well below saturation, the likelihood of finding the QD in a $n \geq 2$ manifold is very small. Detection of a cavity photon, however, increases the conditional probability of finding the QD in a higher manifold, implying in turn that a second photon-emission event is more likely than on average. In contrast, for higher pump powers the average population of excited states is higher and a detection of a cavity photon does not increase the likelihood of a second photon detection event, since the emission of a cavity photon can arise from transitions between any two neighboring excitation manifolds ($n \rightarrow n - 1$ with $n = 2, 3, \ldots$). In this regime, cascaded cavity-photon emission leads to Poissonian statistics.

In order to demonstrate the consistency of our experimental findings and our model, we determine the transition rates between the calculated eigenstates by considering coupling to LO phonons, cavity coupling, and spin-flip processes. The dynamics of the system is then studied by performing a Monte Carlo random walk for a given exci-

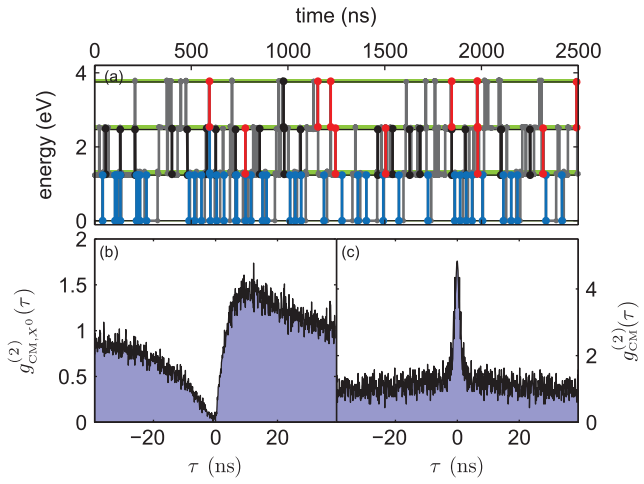

FIG. 4 (color). Simulation of cavity-feeding dynamics. (a) Monte Carlo random walk of excitation and photon-emission events (gray lines). The green horizontal lines correspond to the energy levels presented in Fig. 1(b). Transitions resonant with the CM, X^0, and XX^0 lines are depicted in red, blue, and black, respectively. (b) Extracted CM-X^0 cross-correlation histogram reproducing the characteristic features observed in the experiment [compare Fig. 3(c)]. (c) Extracted CM autocorrelation curve, exhibiting strong bunching at zero time delay in accordance with the experimental result of Fig. 3(e).

tation rate [21,22]. A typical result depicting the system energy as a function of time is shown in Fig. 4(a). Transitions taking place at the cavity-mode frequency are indicated by red lines, whereas X^0 and XX^0 events are shown in blue and black, respectively. Clearly, all cavity photons here are emitted in $2 \rightarrow 1$ and $3 \rightarrow 2$ transitions; in contrast, there are no cavity photons emitted in $1 \rightarrow 0$ transitions, since in that case cavity feeding is energetically not allowed, in perfect agreement with the arguments given above. We remark that our simulation does not include cavity feeding from charged excitonic compounds. However, including charged exciton states would not affect the general validity of the model or our findings.

From the simulated Monte Carlo random walk, we extract both cross-correlation and autocorrelation histograms which are displayed in Figs. 4(b) and 4(c). In the simulation, a CM detuning of 7 meV (5 nm) red of the X^0 was assumed [23]. In general, the experimental observations of Fig. 3 are well reproduced by the simulations. The cross correlation in Fig. 4(b) exhibits the two main features already observed in the experiment: antibunching at zero time delay and a bunching peak for positive times [24]. Figure 4(c) shows a cavity autocorrelation trace for a pump power below saturation. As expected from our qualitative arguments, the curve shows strong bunching with $g^{(2)}_{\mathrm{CM}}(0) \approx 4.8$. In the experiment, however, we only measure $g^{(2)}_{\mathrm{CM}}(0) \approx 1.8$, which we attribute to two effects: first, the experimental pump power is difficult to relate to the theoretical excitation rate and $g^{(2)}_{\mathrm{CM}}(\tau)$ strongly depends on the pump power. Second, in the experiment cavity feeding can additionally arise from charged $1^{\pm} \rightarrow 0^{\pm}$ transitions. Consequently, we expect a reduction of bunching, since here an $n \geq 2^{\pm}$ manifold excitation is not required for cavity feeding.

The work presented here allows for a more refined understanding of QD-based implementations of cavity QED and the limitations of future spin-photon interfaces such devices are predicted to realize. Moreover, it could have strong implications for experiments on lasing [25,26] in such systems. An interesting extension of the present work could be the investigation of feeding in charge-controlled devices [27].

This work is supported by NCCR Quantum Photonics (NCCR QP), research instrument of the Swiss National Science Foundation (SNSF).

[1] G. Khitrova *et al.*, Nature Phys. **2**, 81 (2006).
[2] J. M. Gerard *et al.*, Phys. Rev. Lett. **81**, 1110 (1998).
[3] K. Hennessy *et al.*, Nature (London) **445**, 896 (2007).
[4] M. Kaniber *et al.*, Phys. Rev. B **77**, 161303 (2008).
[5] J. Suffczynski *et al.*, Phys. Rev. Lett. **103**, 027401 (2009).
[6] S. Ates *et al.*, arXiv:0902.3455.
[7] Y. Ota *et al.*, arXiv:0908.0788.
[8] S. Hughes and P. Yao, Opt. Express **17**, 3322 (2009).
[9] M. Yamaguchi, T. Asano, and S. Noda, Opt. Express **16**, 18067 (2008).
[10] U. Hohenester (private communication).
[11] K. Srinivasan and O. Painter, Appl. Phys. Lett. **90**, 031114 (2007).
[12] S. Mosor *et al.*, Appl. Phys. Lett. **87**, 141105 (2005).
[13] M. Winger *et al.*, Phys. Rev. Lett. **101**, 226808 (2008).
[14] E. Biolatti *et al.*, Phys. Rev. B **65**, 075306 (2002).
[15] A. Barenco and M. A. Dupertuis, Phys. Rev. B **52**, 2766 (1995).
[16] C. Gies *et al.*, Phys. Rev. A **75**, 013803 (2007).
[17] K. Karrai *et al.*, Nature (London) **427**, 135 (2004).
[18] We remark here that stability of triplet states in the $n \geq 2$ manifolds against LO-phonon relaxation is likely to play a key role in enhancing cavity feeding from the excited orbital states of the corresponding manifold.
[19] M. Bayer *et al.*, Nature (London) **405**, 923 (2000).
[20] The CM-X^0 cross-correlation curves obtained for another device where the CM was blue detuned with respect to the X^0 line exhibited similar features.
[21] C. Jacoboni and L. Reggiani, Rev. Mod. Phys. **55**, 645 (1983).
[22] M. Grundmann and D. Bimberg, Phys. Rev. B **55**, 9740 (1997).
[23] The truncated continuum of wetting-layer states leads to nonphysical results when going to larger detunings.
[24] Here the bunching feature for $\tau > 0$ is delayed compared to the experimental trace, which could partly be due to the simplified model used for the spin-flip process.
[25] S. Strauf *et al.*, Phys. Rev. Lett. **96**, 127404 (2006).
[26] M. Nomura *et al.*, arXiv:0906.4181.
[27] F. Hofbauer *et al.*, Appl. Phys. Lett. **91**, 201111 (2007).